Letter

First measurement of ^{60}Ge β-decay

A.A. Ciemny[1,a], W. Dominik[1], T. Ginter[2], R. Grzywacz[3,4], Z. Janas[1], M. Kuich[1], C. Mazzocchi[1], K. Miernik[1], M. Pfützner[1], M. Pomorski[1], D. Bazin[2], T. Baumann[2], A. Bezbakh[5], B.P. Crider[2], M. Ćwiok[1], S. Go[3], G. Kamiński[5,6], K. Kolos[3], A. Korgul[1], E. Kwan[2], S.N. Liddick[2,7], S.V. Paulauskas[2,3], J. Pereira[2], K.P. Rykaczewski[4], C. Sumithrarachchi[2], and Y. Xiao[3]

[1] Faculty of Physics, University of Warsaw, 02-093 Warsaw, Poland
[2] National Superconducting Cyclotron Laboratory, Michigan State University, East Lansing, MI 48824, USA
[3] Department of Physics and Astronomy, University of Tennessee, Knoxville, TN 37996, USA
[4] Oak Ridge National Laboratory, Oak Ridge, TN 37831, USA
[5] Joint Institute for Nuclear Research, 141980 Dubna, Russia
[6] Institute of Nuclear Physics PAN, 31-342 Cracow, Poland
[7] Department of Chemistry, Michigan State University, East Lansing, MI 48824, USA

Abstract. The $N = 28$ isotone ^{60}Ge, $T_z = -2$, was produced and selected among the products of the fragmentation reaction of a ^{78}Kr beam at $150\,\mathrm{MeV/nucleon}$ and a Be target by means of the A1900 fragment separator at the National Superconducting Cyclotron Laboratory (NSCL) at Michigan State University (MSU). Its decay was studied for the first time using the optical time projection chamber. The β-decay of ^{60}Ge was found to be dominated by β-delayed proton emission, with a branching of $\approx 100\%$ and half-life $T_{1/2} = 20^{+7}_{-5}\,\mathrm{ms}$.

1 Introduction

Exploring the properties of the nuclei lying far from the β-stability path is an important topic of nuclear physics studies. Experimental measurements that allow estimate of the binding energies and half-lives for β-decay on the proton-rich side of the chart of nuclei are crucial for astrophysics, as the competition between β-decay and particle capture shapes the rp-process path. The latter impacts the abundance of heavy elements in the universe [1,2]. On the other hand, the comparison of experimental studies with theory yields important information about the validity of models for nuclear structure and interactions between the nucleons themselves. This is particularly crucial for exotic nuclei close to the nucleon drip-lines.

The region around and above ^{48}Ni is very interesting from the nuclear structure point of view. One of the questions is how the structure of proton drip-line nuclei changes when pairs of protons are added to the closed proton shell. While the study of the two-proton radioactivity provided the first glimpses of the properties of ^{48}Ni ($Z = 28$) [3] and ^{54}Zn ($Z = 30$) [4], the next system of interest is ^{60}Ge ($Z = 32$) which is special in this context because of the closed neutron shell, $N = 28$. The comparison between ^{48}Ni and ^{60}Ge may shed light on proton cor-

relation effects in this region. Additionally, ^{60}Ge appears to be the heaviest semi-magic nucleus for which the mirror symmetry can be studied —its isospin conjugate system is the stable ^{60}Ni. Finally, the question arises whether $N = 28$ is still a magic number at ^{60}Ge. Unfortunately, the spectroscopic information on nuclei in this region is scarce. ^{60}Ge was discovered more than 10 years ago, when three atoms of this isotope were identified at the NSCL at MSU [5], but nothing was known on its decay. Based on the fact that they survived the time of flight through the A1900 separator, only a lower limit for the half-life was estimated to be $110\,\mathrm{ns}$ [5]. Until recently, ^{60}Ge was the most neutron-deficient germanium isotope known [6].

The ^{60}Ge nucleus is predicted to be stable against one- and two-proton emission [2]. The β-decay energy is estimated to be $Q_{EC} = 12180(280)\,\mathrm{keV}$ [7]. The separation energies for the one, two, and three protons in ^{60}Ga, the β^+ daughter nucleus of ^{60}Ge, are predicted to be, $-140(200)\,\mathrm{keV}$, $2700(200)\,\mathrm{keV}$ and $5570(200)\,\mathrm{keV}$ [7], respectively. Thus, several channels for β-delayed (multi)-proton emission are open, and in fact delayed proton emission is expected to dominate the decay of ^{60}Ge.

Here we report on the very first information on the decay of ^{60}Ge. It was obtained in the same experiment which yielded the first observation of ^{59}Ge, already reported in [6].

a e-mail: aleksandra.ciemny@fuw.edu.pl

2 Experimental technique

The experiment was performed at the National Superconducting Cyclotron Laboratory at Michigan State University. The most neutron-deficient isotopes of germanium were produced in the fragmentation reaction of a primary beam of $^{78}Kr^{34+}$ ions at $150\,MeV/nucleon$ impinging on a $200\,mg/cm^2$ Be target. The ions of interest were separated from the other reaction products by means of the A1900 separator [8]. The ion optics setting of the A1900 separator and the achromatic aluminium degrader placed at the intermediate focal plane (thickness $384\,mg/cm^2$) were optimized for the transmission of ^{60}Ge. The ions of ^{60}Ge were transmitted from the focal plane of the A1900 spectrometer to the experimental vault where they were stopped in the active volume of the Optical Time Projection Chamber (OTPC) [3], where they decayed. In brief, the active volume of this gaseous detector, $33 \times 20 \times 21\,cm^3$ (depth, width, and height, respectively), is immersed in a homogeneous electric field. The ion enters the detector horizontally, perpendicular to the electric field lines. In the detector, the ion and the charged decay products (protons, alphas) ionize the gas. The electrons generated in the process drift downwards, towards the anode, where they are multiplied by a series of four Gas Electron Multiplier (GEM) foils. The light generated in this process is detected by a photomultiplier (PMT) and a CCD camera. The image collected by the CCD camera gives the projection of the trajectory on the plane perpendicular to the field lines (xy), while the PMT gives the time distribution of the signals. The latter allows reconstruction of the third dimension (z) for the trajectories, if the drift velocity of the electrons is known for the gas mixture used. In this experiment, the gas mixture was 49.5% He $+ 49.5\%$ Ar $+ 1\%$ CO_2 at atmospheric pressure. The drift velocity of the electrons in the gas was measured to be $v_{drift} = 1.05(1)\,cm \cdot \mu s^{-1}$. The sensitivity of the detector can be adjusted by a special gating electrode mounted between the drift volume and the amplifying section. While waiting for a triggering ion, the potential of this electrode is set to a value that allows the observation of highly-ionising heavy ions without overloading the amplification stage ("low-sensitivity mode"). Upon receiving a trigger, this potential is changed within $100\,\mu s$ to the "high-sensitivity" mode which allows the detection of a much weaker ionisation due to low-energy light particles, like protons.

Each fragment transmitted to the experimental vault was identified on an event-by-event basis by means of its energy loss (ΔE) in a Si detector placed in the front of the OTPC and the time of flight (ToF) between a scintillator placed at the A1900 focal plane and another scintillator positioned downstream from it (see fig. 1 in ref. [6]). The data acquisition system handled the CCD image and the PMT, ΔE and ToF signals read out by digital oscilloscopes. Hardware gates were imposed on both ΔE and ToF signals and adjusted to select all of the ^{60}Ge ions and part of the ^{58}Zn ions (see fig. 1). A trigger was generated from these signals to constrain the amount of data to be recorded.
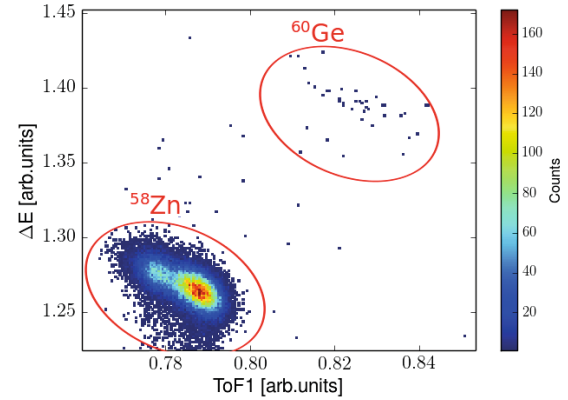

Fig. 1. (Color online) Identification plot for ions that triggered the OTPC detector. The red ellipses of identical size are used to highlight ^{60}Ge and ^{58}Zn events.

The OTPC was operated in the so-called "extended exposure" mode [3]. The CCD camera took images continuously with a constant exposure time (implantation gate, $\sim 20\,ms$), during which the OTPC was kept in the "low-sensitivity" regime. When the trigger signal was generated, the exposure time was extended by $100\,ms$ (decay gate) and the primary beam was turned off for the same duration to prevent other ions from entering the detector while waiting for the decay of the triggering ion. During this time the OTPC was operated in the "high-sensitivity" regime. For each event, the PMT waveform from the beginning of the last implantation gate before the trigger until the end of the corresponding decay gate was recorded by a digital oscilloscope.

3 Results and discussion

Figure 1 shows the ΔE-ToF identification plot for the triggering ions, the A1900 optimized for ^{60}Ge. A total of 41 events of ^{60}Ge ions were identified in the OTPC data acquisition system. Out of them, 28 were implanted in the active volume of the OTPC. An ion was classified as implanted if it was stopped between 10% and 90% of the depth of the chamber. This restriction was necessary to ensure that no proton escaped through the wall of the chamber without being registered. The other ions either stopped close to the edge of the active part of the detector or outside it. This was due to the fact that the range distribution of projectile fragments was broader than the active thickness of the detector. The observed stopping efficiency was found to be consistent with the LISE++ simulations of the setup [9].

Each ^{60}Ge event has been analysed to search for the emission of delayed particles. In 19 events, the decay by emission of a single delayed proton (βp) was observed. In fig. 2, an example event of a ^{60}Ge implanted ion followed by βp emission is shown. The time between the arrival of an ion and the emission of the proton, recorded by the PMT, was measured for every decay event. From this data the half-life of ^{60}Ge was determined to be $T_{1/2} = 20^{+7}_{-5}\,ms$
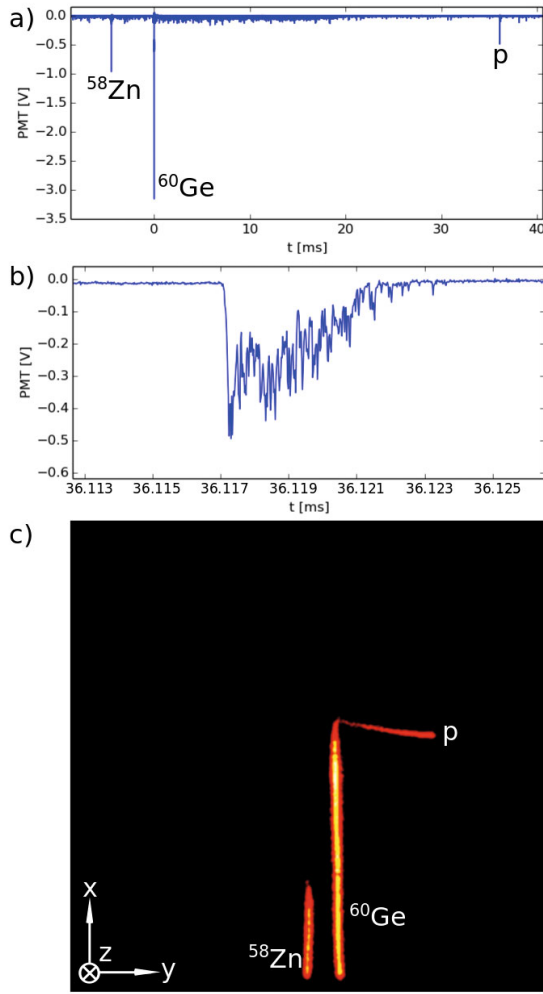
Fig. 2. (Color online) Example event with βp emission from ^{60}Ge. (a) Light intensity *versus* time for the PMT signal. At $t = 0$ ms the ^{60}Ge ion arrived and triggered the acquisition system. At $t = 36.12$ ms a decay occurred with the emission of a proton. Also the signal from the non-triggering ^{58}Zn ion (not a known βp emitter) is visible. This ion entered the chamber during the implantation gate, 4.5 ms before the trigger. (b) PMT signal of the proton, zoomed. (c) CCD image showing two bright tracks due to ions and a track of the proton.

by the maximum likelihood method using an exponential decay distribution with a finite-time window for the observation of the decay [10]. The dead time after the trigger due to the sensitivity change in the detector is about $100\,\mu$s. Figure 3 shows the decay-time distribution of the ^{60}Ge events on a logarithmic time-scale.

From the Coulomb-energy-difference systematics [11] for isospin $T = 2$, we calculate the decay energy to the isobaric analogue state (IAS) equal to 9664(6) keV. Then the partial half-life for the Fermi (F) decay of ^{60}Ge is $T_{1/2}^{F} \cong 44$ ms [12]. In addition, we have to take into account the Gamow-Teller (GT) transitions. In ref. [13] the extensive calculations of GT transitions were reported using the finite-range droplet model (FRDM) and
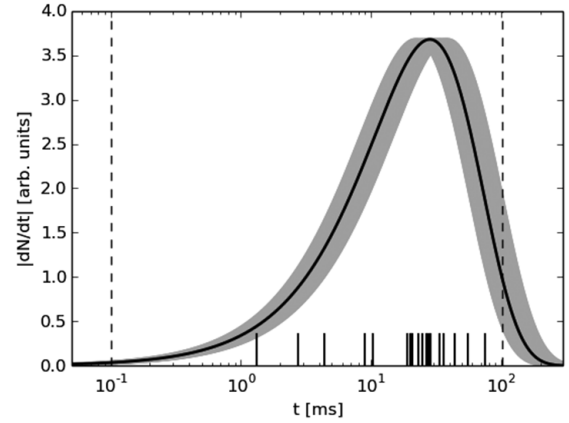
Fig. 3. Logarithmic decay-time distribution ($|\mathrm{d}N/\mathrm{d}t|$) for the events of ^{60}Ge. The bell-shaped curve is the distribution calculated for $T_{1/2} = 20$ ms [14] and the grey area represents its uncertainty. Each event measured is represented by a black vertical bar. The dashed lines show the observation-window during the experiment.

Table 1. Theoretical predictions for the β^{+}-decay half-life of ^{60}Ge and the experimental result from this work. The value from ref. [13] is combined with our estimate of the Fermi transition. Calculations from ref. [15] are given for three different mass models. See text for details.

Möller [13] + F	Hirsch [15]		This exp.
$T_{1/2}$ [ms]	Mass-formula	$T_{1/2}$ [ms]	$T_{1/2}$ [ms]
	Hilf [16]	34.6	
29	Groote [17]	31.3	20^{+7}_{-5}
	Möller [18]	32.3	

the folded-Yukawa single-particle potential combined with quasi-particle random phase approximation (QRPA). The prediction for ^{60}Ge is $T_{1/2}^{GT} = 82$ ms [13]. From these two values we obtain $T_{1/2} = [(T_{1/2}^{F})^{-1} + (T_{1/2}^{GT})^{-1}]^{-1} \cong 29$ ms. It is within 2σ of our measured value. Microscopic calculations by Hirsch *et al.* [15] for β^{+}/EC decay half-lives for neutron-deficient nuclei using the proton-neutron quasi-particle random phase approximation (pn-QRPA) with both particle-hole and particle-particle residual interaction included, also take into account both Fermi and GT transitions. Their predictions for the half-life of ^{60}Ge, obtained with three different mass models, are between 31.3 and 34.6 ms, also in a fair agreement with experiment. The calculated half-lives and the result of our measurement are summarised in table 1.

Out of the 19 protons observed, 11 were stopped in the active volume of the detector. This is demonstrated by the fact that they show the structure of the Bragg peak in the PMT signal and in the CCD image (see, *e.g.*, fig. 2(b) and (c)). In all these cases the proton trajectories are oriented downwards (towards the anode). In the remaining 8 cases, the Bragg peak is not clearly visible. This might happen when the trajectory is almost horizon-

tal (parallel to the electrodes) or the proton is not stopped in the active volume of the detector. Not a single proton trajectory clearly directed towards the top of the chamber (cathode) was observed. Such an effect can be explained if the ^{60}Ge ion drifts towards the cathode before being neutralized and there it later decays. Since the emission of the protons happens at the cathode, only protons emitted downwards can be fully observed in the active volume of the detector. Assuming this scenario and the isotropic emission of β-delayed protons, the efficiency for detecting protons is about 50%. For estimating the branching ratio we take into account all 11 clearly downwards-emitted protons and 4 protons out of the 8 with unknown direction. This leads to the value of the branching ratio for the βp emission consistent with 100%, as expected for the decay of ^{60}Ge.

For ions decaying at the upper wall of the detector, the probability to observe two protons is about 1/4, if no correlation between these protons is assumed. Since we did not see any such event, we can only set an approximate upper limit for the branching ratio for the $\beta 2p$ emission, $b_{\beta 2p} < 14\%$. We note, however, that there are reasons for this branching ratio to be small. From the Coulomb-energy difference discussed above [11] and the decay energy Q_{EC}, it follows that the IAS state is located in ^{60}Ga at an excitation energy of only 2520(280) keV, which is below the two-proton separation energy. Moreover, the level scheme of ^{60}Cu, the ^{60}Ga mirror nucleus, suggests that several 1^+ states are available at low excitation energy (below the 2.5 MeV IAS) for GT decay of the 0^+ ground state of ^{60}Ge. Then, the β-delayed multi-proton emission would require a sizeable β strength at excitation energies well above the IAS.

4 Summary

β-decay of ^{60}Ge was measured for the first time at the National Superconducting Cyclotron Laboratory at Michigan State University by means of the OTPC detector. Events with βp emission were observed and the β-decay half-life of this isotope is $T_{1/2} = 20^{+7}_{-5}$ ms. This value is in good agreement with theoretical predictions accounting for allowed β transitions of F and GT type. The branching ratio for βp emission in ^{60}Ge was found to be compatible with 100%. More in depth studies will require higher statistics, in order to measure the energy spectrum of β-delayed protons and to search for β-delayed multi-proton emission.

References

1. H. Schatz *et al.*, Phys. Rep. **294**, 167 (1998).
2. B.A. Brown *et al.*, Phys. Rev. C **65**, 045802 (2002).
3. M. Pomorski *et al.*, Phys. Rev. C **90**, 014311 (2014).
4. P. Ascher *et al.*, Phys. Rev. Lett. **107**, 102502 (2011).
5. A. Stolz *et al.*, Phys. Lett. B **627**, 32 (2005).
6. A.A. Ciemny *et al.*, Phys. Rev. C **92**, 014622 (2015).
7. M. Wang *et al.*, Chin. Phys. C **36**, 1603 (2012).
8. D.J. Morrissey *et al.*, Nucl. Instrum. Methods Phys. Res. B **204**, 90 (2003).
9. www.lise.nscl.msu.edu.
10. K. Miernik, Acta Phys. Pol. B **46**, 725 (2015).
11. M.S. Antony, A. Pape, J. Britz, At. Data Nucl. Data Tables **66**, 1 (1997).
12. K. Grotz, H.V. Klapdor, *The Weak Interaction in Nuclear, Particle and Astrophysics* (Adam Hilger, New York, 1990).
13. P. Möller, J.R. Nix, K.-L. Kratz, At. Data Nucl. Data Tables **66**, 131 (1997).
14. K.H. Schmidt, Eur. Phys. J. A **8**, 141 (2000).
15. M. Hirsch *et al.*, At. Data Nucl. Data Tables **53**, 165 (1993).
16. E.R. Hilf, H.v. Groote, K. Takahashi, CERN Report No. 76-13 (1976), p. 142.
17. H.v. Groote, E.R. Hilf, K. Takahashi, At. Data Nucl. Data Tables **17**, 418 (1976).
18. P. Möller, J.R. Nix, At. Data Nucl. Data Tables **26**, 165 (1981).